

Preparation and Chiral Recognition of Polysaccharide-Based Selectors

Tomoyuki Ikai and Yoshio Okamoto

Contents

1	Introduction	34
2	Preparation and Chiral Recognition of Polysaccharide Chiral Selectors	35
2.1	Polysaccharide Esters	35
2.2	Polysaccharide Phenylcarbamates	37
3	Structural Analysis of Phenylcarbamate Derivatives of Cellulose and Amylose	39
4	Chiral Recognition Mechanism	40
4.1	NMR Studies	40
4.2	Computational Methods	46
4.3	Other Studies for Chiral Recognition Mechanism	48
5	Conclusions	49
	References	50

Abstract Among more than one hundred commercially available CSPs, those based on the phenylcarbamates of polysaccharides including cellulose and amylose have been recognized as the most powerful for the resolution of a wide range of racemates, and nearly 90% of chiral compounds can be resolved at the analytical level using the polysaccharide-based CSPs. Although the qualitative understanding of the chiral recognition mechanism of polysaccharide-based CSPs is rather difficult in contrast to the small molecule-based CSPs, several attempts have made for comprehension of the chromatographic behavior on the polysaccharide-based CSPs. In this chapter, after describing the development of the polysaccharide-based CSPs with high recognition ability, special emphasis is placed on the mechanistic study of the polysaccharide-based CSPs on the basis of spectroscopic and computational methods.

Y. Okamoto (✉)

Nagoya University, Furo-cho, Chikusa-ku, Nagoya 464-8603, Japan
e-mail: okamoto@apchem.nagoya-u.ac.jp

1 Introduction

The development of chiral stationary phases (CSPs) for high-performance liquid chromatography (HPLC) with high recognition ability, wide applicability, and high loading capacity has attracted a lot of attention, and the number of commercially available CSPs has surpassed one hundred. These CSPs for HPLC have been prepared using both chiral small molecules and polymers with chiral recognition abilities.

In 1971, Davankov et al. achieved the first baseline separation of enantiomers using a small molecule-based CSP consisting of L-proline [1]. Since then, a wide range of chiral small compounds, which include amino acids, cyclodextrins, macrocyclic glycopeptides, cinchona alkaloids, crown ethers, π -basic or π -acidic aromatic compounds, etc., have been used as CSPs [2–6]. On the other hand, the polymer-based CSPs are further divided into two categories, i.e., synthetic and natural chiral polymers [7, 8]. Typical examples of the synthetic polymers are molecularly imprinted polymer gels, poly(meth)acrylamides, polymethacrylates, polymaleimides, and polyamides, and those of the natural polymers include polysaccharide derivatives and proteins.

Figure 1 shows the distribution of the CSPs for HPLC used for the determination of enantiomeric excess (*ee*) that was reported in the *Journal of the American Chemical Society* in 2005 (a) and 2007 (b) [2, 9]. These statistics show that more than 90% of the *ee* determinations by chiral HPLC are carried out by the polysaccharide-based CSPs.

However, the chiral recognition mechanism of the polysaccharide-based CSPs at a molecular level has not yet been completely clarified. In contrast to the small molecule-based CSPs, the understanding of the chiral recognition mechanism of polymer-based CSPs is usually difficult. This is because a variety of interaction sites with different affinities for enantiomers exist in chiral polymer chains, and the

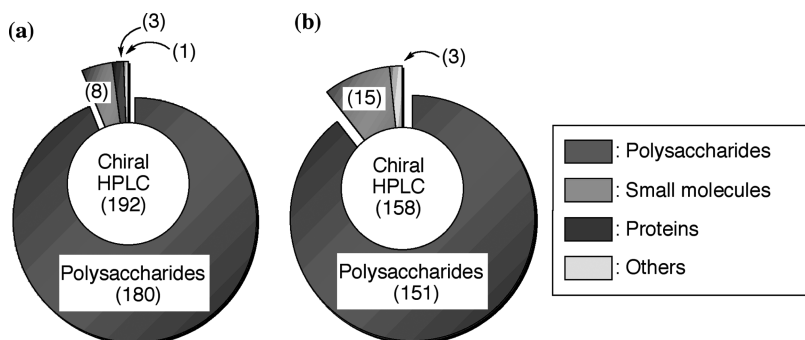


Fig. 1 Distribution of CSPs for HPLC used for the determination of enantiomeric excess reported in *Journal of the American Chemical Society* in (a) 2005 and (b) 2007. The values in parentheses represent the number of the counted papers. Reprinted by permission from the Royal Society of Chemistry [2] and International Union of Pure and Applied Chemistry [9]

determination of their precise structures both in the solid and in the solution states is not easy.

In this chapter, we will describe the development and chiral recognition mechanism of polysaccharide-based CSPs capable of the efficient separation of enantiomers. First, the development of the polysaccharide-based CSPs with a high-recognition ability is briefly described, and then special emphasis will be placed on the mechanistic study of the polysaccharide-based CSPs on the basis of spectroscopic and computational investigations.

2 Preparation and Chiral Recognition of Polysaccharide Chiral Selectors

2.1 Polysaccharide Esters

Polysaccharides, such as cellulose **1** and amylose **2**, are the most abundant natural polymer resources on the earth and are optically active (Fig. 2). Although the native polysaccharides themselves can discriminate enantiomers and resolve several racemic compounds by liquid chromatography [10–12], their recognition abilities are not sufficiently adequate to be practically used as CSPs. More useful CSPs can be obtained through modification of the polysaccharides. In 1973, the first practical CSP derived from polysaccharides was reported by Hesse and Hagel [13]. They found that the microcrystalline cellulose triacetate, CTA-1 (**3** in Fig. 3), which was synthesized by the heterogeneous acetylation of the native microcrystalline cellulose, showed a useful recognition ability during liquid chromatography. The crystalline structure of CTA-1 is expected to maintain that of the native cellulose and the chiral recognition ability seems to be derived from its crystalline structure. Therefore, once CTA-I is dissolved in a solvent, its recognition ability is completely changed from that of CTA-I. For example, the opposite elution order of

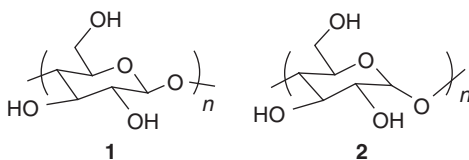


Fig. 2 Structures of cellulose (**1**) and amylose (**2**)

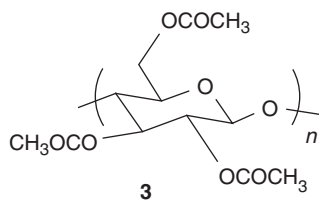


Fig. 3 Structure of cellulose triacetate **3** (CTA-1)

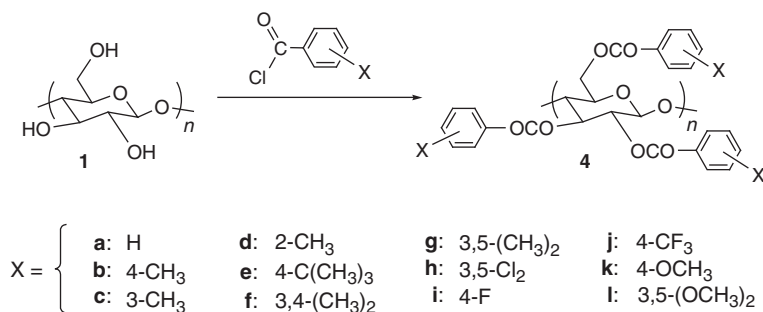


Fig. 4 Synthesis and structure of cellulose benzoates **4**

the enantiomers of Tröger base was observed using two kinds of cellulose triacetate-based CSPs [14]. The difference in the recognition seems to be derived from the change in its structure.

Since the microcrystalline cellulose triacetate CTA-1 was recognized as a practical CSP in the 1970s, various kinds of cellulose esters have been prepared to evaluate their recognition abilities as CSPs for HPLC [14–16]. Among them, the cellulose benzoates (**4** in Fig. 4), which are easily obtained by reacting cellulose with the corresponding benzoyl chlorides, show high-recognition abilities when they are coated on silica gel. The effect of the substituents on the phenyl group, which include alkyl, halogen, trifluoromethyl, and methoxy groups, has been systematically studied [16]. The benzoate derivatives with electron-donating substituents, such as an alkyl group, have a tendency to show a higher recognition ability than those with electron-withdrawing substituents, such as a halogen and trifluoromethyl. The most likely reason for this observation is that the electron density of the carbonyl groups of the cellulose derivatives is significantly influenced through an inductive effect of the substituents on the phenyl groups. However, the electron-donating methoxy group does not work to increase the recognition ability due to the high polarity of the substituent itself. Among these cellulose benzoates, 4-methylbenzoate **4b** exhibits an especially high chiral recognition ability and has been used for the resolutions of a broad range of chiral compounds [17, 18]. In contrast to the cellulose derivatives **4**, the amylose benzoates (**5** in Fig. 5) show almost no recognition abilities as CSPs. This may be due to the lower conformational stability of the amylose derivatives, which causes many conformational isomers to be formed.

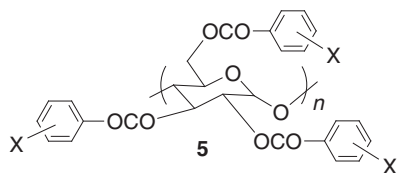


Fig. 5 Structure of amylose benzoates **5**

2.2 Polysaccharide Phenylcarbamates

Cellulose (**1**) and amylose (**2**) are readily converted to various phenylcarbamate derivatives (**6** and **7**) by reacting them with the corresponding phenyl isocyanates (Fig. 6) [19, 20]. The recognition abilities of these derivatives can be significantly changed, depending on the substituents on the phenyl groups as well as the benzoate derivatives. The resolution results of 10 racemates **8–17** (Fig. 7) on the nine *para*-substituted phenylcarbamates of cellulose are given in Table 1, in which the substituents on the phenyl group are arranged in the order of their increasing electron-donating powers from left to right [20]. In addition, the retention times of acetone and the first isomer of alcohol **16** eluted on the *para*-substituted CSPs are plotted versus the Hammett parameter σ of the substituents (Fig. 8).

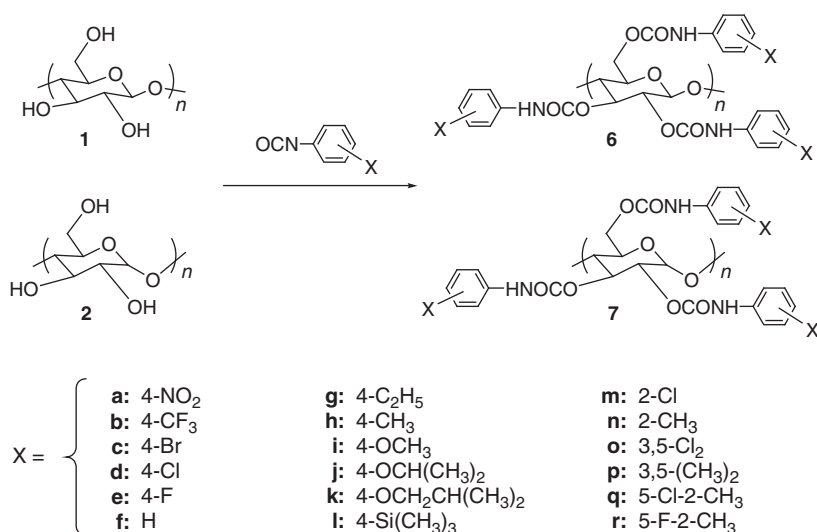


Fig. 6 Synthesis and structures of phenylcarbamate derivatives of cellulose **6** and amylose **7**

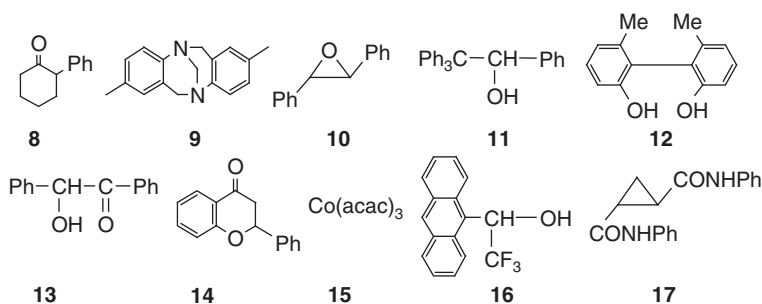
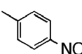
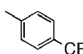
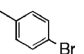
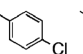
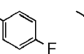
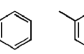
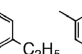
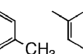



Fig. 7 Structures of racemates **8–17**

Table 1. Separation factors (α) on the *para*-substituted phenylcarbamates of cellulose

									
Racemates	6a	6b	6c	6d	6e	6f	6g	6h	6i
8	~1 (-)	1.18 (-)	1.17 (-)	1.16 (-)	1.12 (-)	1.17 (-)	1.19 (-)	1.20 (-)	1.13 (-)
9	~1 (-)	1.23 (+)	1.19 (+)	1.16 (+)	1.14 (+)	1.37 (+)	1.11 (+)	1.48 (+)	~1 (+)
10	1.33 (+)	1.61 (+)	1.70 (+)	1.68 (+)	1.38 (+)	1.46 (+)	1.55 (+)	1.55 (+)	1.34 (+)
11	1.00	1.48 (+)	1.95 (+)	1.95 (+)	1.64 (+)	1.22 (+)	1.59 (+)	1.37 (+)	1.00
12	~1 (+)	2.04 (-)	1.21 (-)	1.20 (-)	1.17 (-)	1.65 (-)	1.33 (-)	1.30 (-)	1.15 (-)
13	1.00	1.10 (-)	1.13 (-)	1.20 (-)	1.14 (-)	~1 (+)	1.14 (-)	1.12 (-)	~1 (+)
14	1.00	1.14 (+)	1.13 (+)	1.12 (+)	1.13 (+)	1.10 (+)	1.22 (-)	1.16 (+)	~1 (+)
15	~1 (+)	2.06 (+)	1.79 (+)	1.46 (+)	1.53 (+)	1.24 (+)	1.76 (+)	1.75 (+)	~1 (+)
16	~1 (+)	1.30 (-)	1.29 (-)	1.29 (-)	1.26 (-)	1.45 (-)	1.57 (-)	1.52 (-)	1.35 (-)
17	~1 (+)	1.22 (-)	1.17 (-)	1.44 (-)	~1 (-)	1.45 (-)	2.12 (-)	1.35 (-)	1.00

Column: 25×0.46 cm (i.d.). Flow rate: 0.5 ml/min. Eluent: hexane–2-propanol (90:10). The signs in parentheses represent the optical rotation of the first-eluted enantiomer.

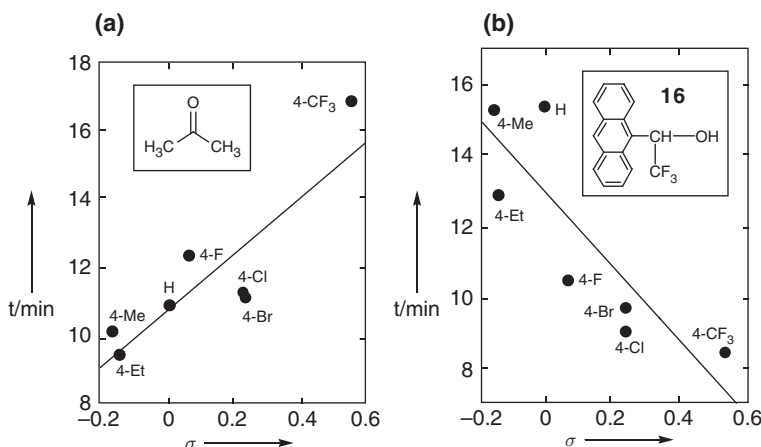


Fig. 8 Plots of retention times t of (a) acetone and (b) the first enantiomer of **16** to elute on cellulose phenylcarbamate derivatives against the Hammett parameter σ of the substituents. Reprinted by permission from Elsevier [20]

Compared to the non-substituted cellulose derivative **6f**, the phenylcarbamates bearing electron-withdrawing substituents, such as halogens, or electron-donating substituents, such as alkyl groups, exhibit better chiral recognitions. These substituents appear to affect the polarity of the carbamate group via an inductive effect and alter the interaction mode between the cellulose derivatives and the racemates.

When the electron-withdrawing groups are substituted on the phenyl groups, the acidity of the NH proton of the carbamate groups increases. Therefore, the retention time of acetone on the CSPs with the electron-withdrawing groups is increased, because acetone is mainly adsorbed on the derivatives through a hydrogen-bonding interaction with the NH groups. On the contrary, as the electron-donating power of the substituents on the phenyl group becomes more intensive, the electron density at the carbonyl oxygen of the carbamate groups must be increased, and the racemate

16 is more strongly adsorbed on the derivatives through hydrogen bonding with the carbonyl groups. On the other hand, the derivatives bearing fairly polar substituents on the phenyl groups, such as the nitro (**6a**) or methoxy (**6i**) groups, exhibit a rather low recognition ability. Because the nitro or methoxy group is located far from a chiral glucose unit, these polar groups themselves are expected to cause a non-enantioselective interaction with the racemates. Therefore, the introductions of bulky alkoxy groups, such as isopropoxy (**6j**) or isobutoxy (**6k**) groups, instead of the methoxy group can improve the recognition ability by preventing the non-enantioselective interactions at the ether oxygen atom [21].

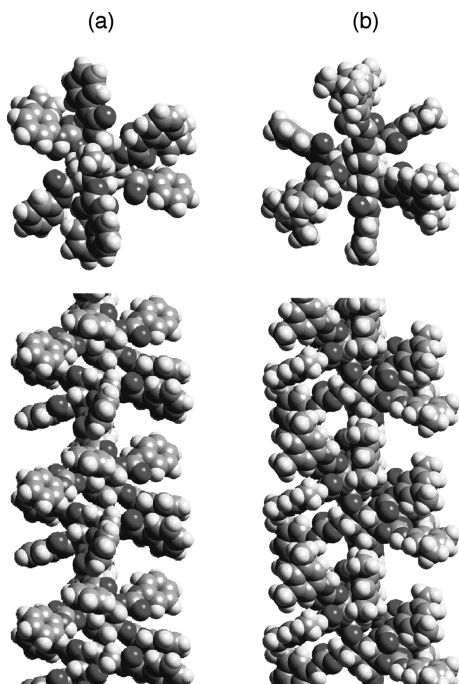
The chiral recognition on the cellulose phenylcarbamates is also influenced by the position of the substituents on the phenyl group. When a halogen or methyl group is introduced at an *ortho* position (**6m**, **6n**), the recognition ability significantly decreases compared to the non-substituted cellulose derivative (**6f**) [22]. Most cellulose phenylcarbamates with a high-recognition ability form a lyotropic liquid crystalline phase in a highly concentrated solution [20]. This indicates that the phenylcarbamates as the CSPs are presumably arranged in a regular fashion. Such an ordered structure seems to be important for efficient chiral recognition on polymer-based CSPs. However, the *ortho*-substituted derivatives (**6m**, **6n**) do not show such a liquid crystallinity. This means that the *ortho*-substituted derivatives may not possess a regular higher-order structure.

For amylose phenylcarbamates **7** (Fig. 6), the introduction of chloro or methyl groups on the phenyl groups also has a meaningful effect on their recognition ability [23–25]. In contrast to the cellulose derivatives, however, amylose derivatives with substituents at the *ortho* position, such as the 5-chloro-2-methyl- (**7q**) and 5-fluoro-2-methylphenylcarbamates (**7r**), exhibit a relatively high-recognition ability [24, 25]. The difference in the substituent effect on their chiral recognition may be derived from the difference in their higher order structures.

3 Structural Analysis of Phenylcarbamate Derivatives of Cellulose and Amylose

The intimate structural analysis of the polysaccharide derivatives is mandatory in order to clarify the chiral recognition mechanism. Figure 9 shows the stable structures of **6f** and **6p**, which were optimized by molecular-mechanics calculations starting from the proposed X-ray crystal structure of **6f** [26]. These derivatives have similar left-handed 3/2-helical conformations, and the glucose residues are regularly arranged along the helical axis. A chiral helical groove with polar carbamate groups exists parallel to the main chain. The polar carbamate groups are preferably located inside, and hydrophobic aromatic groups are placed outside the polymer chain so that polar racemates may predominately interact with the carbamate residues through hydrogen-bonding and dipole–dipole interactions. These interactions seem to be significant for efficient chiral recognition, especially in normal-phase HPLC using nonpolar eluents. This speculation is supported by NMR studies as described below. Besides these polar interactions, π – π interactions between the phenyl groups

Fig. 9 Optimized structures of (a) phenylcarbamate **6f** and (b) 3,5-dimethylphenylcarbamate **6p** of cellulose. Perpendicular (*top*) and along (*bottom*) to the helix axis. Reprinted by permission from The Chemical Society of Japan [26]



of the phenylcarbamates and an aromatic group of a racemate may also play an important role in their recognitions, because several aromatic compounds without any polar groups can also be resolved particularly in reversed-phase mode HPLC with polar eluents.

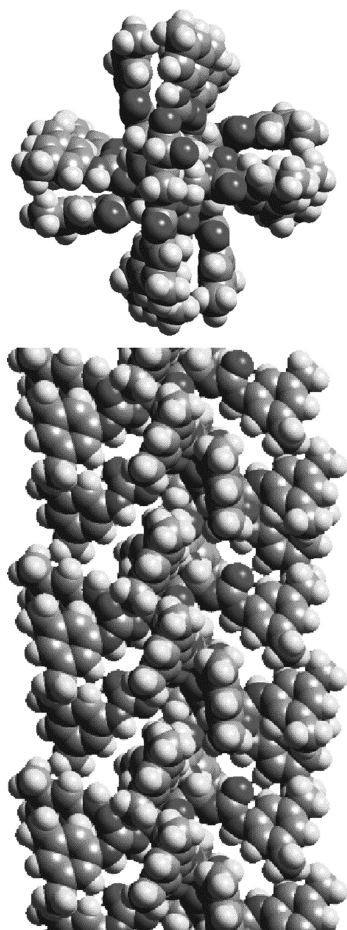
Meanwhile, the structures of the amylose phenylcarbamate derivatives have not yet been determined by X-ray studies. Wang et al. investigated the structure of **7p** by solid-state NMR and pointed out that **7p** forms a helical structure with less than six-folds in the solid state [27]. Recently, we investigated the structure of **7p**, which had a low degree of polymerization and was soluble in chloroform, by the combination technique involving 2D NMR and computer modeling [28]. Figure 10 shows the optimized structure of **7p** with a left-handed 4/3 helix as the most probable one. Similar to the cellulose derivatives, the polar carbamate groups are located inside the polymer chain and the aromatic groups are on the outside.

4 Chiral Recognition Mechanism

4.1 NMR Studies

NMR spectroscopy is well known to be one of the most powerful tools for the elucidation of the chiral recognition mechanism on a molecular level. Most carbamate

Fig. 10 Optimized structures of amylose 3,5-dimethylphenylcarbamate **7p**. Perpendicular (*top*) and along (*bottom*) to the helix axis. Reprinted by permission from American Chemical Society [28]

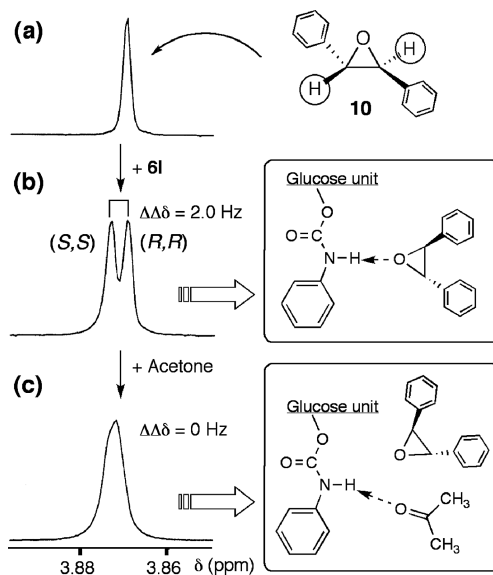


derivatives with high-recognition abilities are soluble only in polar organic solvents, such as tetrahydrofuran (THF), acetone, pyridine, dimethyl sulfoxide, etc. In these solvents, the polysaccharide derivatives cannot have a sufficient interaction with enantiomers for efficient recognition due to the stronger interaction between the polysaccharide derivatives and the solvent molecules. Therefore, it is difficult to reveal the chiral recognition mechanism on polysaccharide-based selectors by NMR spectroscopy. In the past 15 years, however, it was found that several carbamate derivatives, such as 4-trimethylsilylphenyl- (**6l**) [29–31], 3,5-dichlorophenyl- (**6o**) [30], 5-fluoro-2-methylphenyl- (**6r**) [32], and cyclohexylcarbamate [33], are soluble in chloroform and can discriminate enantiomers by NMR spectroscopy as well as by HPLC.

Figure 11 shows the 500 MHz ^1H NMR spectra of *rac-trans*-stilbene oxide **10** with and without cellulose 4-trimethylsilylphenylcarbamate **6l** in CDCl_3 [29–31]. The methine proton resonance of the enantiomer **10** was apparently separated into

Fig. 11 ^1H NMR spectra of *rac*-**10** in the presence of **6l** in CDCl_3 (1.0 ml). **6l**: (a) 0 and (b and c) 20 mg, acetone: (a and b) 0 and (c) 65 μL .

Reprinted by permission from The Chemical Society of Japan [29]



two sets of peaks in the presence of **6l**, and only the resonance of the (*S,S*)-isomer is downfield shifted. The chemical shift difference ($\Delta\Delta\delta$) of these two peaks increased with a decrease in temperature and with an increase in the amount of **6l**. This indicates that **6l** can recognize the enantiomers even in solution. Because the most important adsorption site for chiral recognition on the phenylcarbamate derivatives must be the polar carbamate groups, the oxygen atom of the oxirane ring in **10** may interact with the NH proton of the carbamate group through a hydrogen bond. Therefore, the addition of acetone, which is a hydrogen-bonding acceptor and attenuates the interaction between **10** and **6l** by hydrogen bonding with the NH proton, causes the splitting of the methine proton resonance to disappear. Many other racemates can be also recognized on **6l** in CDCl_3 [30].

The cellulose derivative **6r** can also discriminate the enantiomers of **18** by ^1H NMR spectroscopy [32]. Figure 12 shows the ^1H NMR spectra of *rac*-**18** in the absence (a) and presence (b) of **6r** in CDCl_3 . Each signal for the hydroxyl and naphthyl (H4 and H6) protons of **18** is clearly split into two sets of peaks due to the enantiomers. The signals for the hydroxy protons of (*S*)-**18** are more downfield shifted with peak broadening than that for (*R*)-**18**, while the signals for the H4 and H6 protons of (*S*)-**18** are upfield shifted with broadening. This means that (*S*)-**18** has a stronger interaction with **6r**. The downfield shift of the hydroxy protons is presumably due to hydrogen bonding between the carbamate group of the cellulose derivative and the hydroxy group of (*S*)-**18**, and the upfield shifts of the aromatic protons may be ascribed to the π -stacking or shielding effect of an adjacent aromatic ring of **6r**. During the HPLC separation of *rac*-**18** on **6r**, the (*R*)-isomer is first eluted followed by the (*S*)-isomer ($\alpha = 4.23$) (Fig. 13). This HPLC elution order agrees with the large shifts in the (*S*)-isomer observed in the ^1H NMR spectrum.

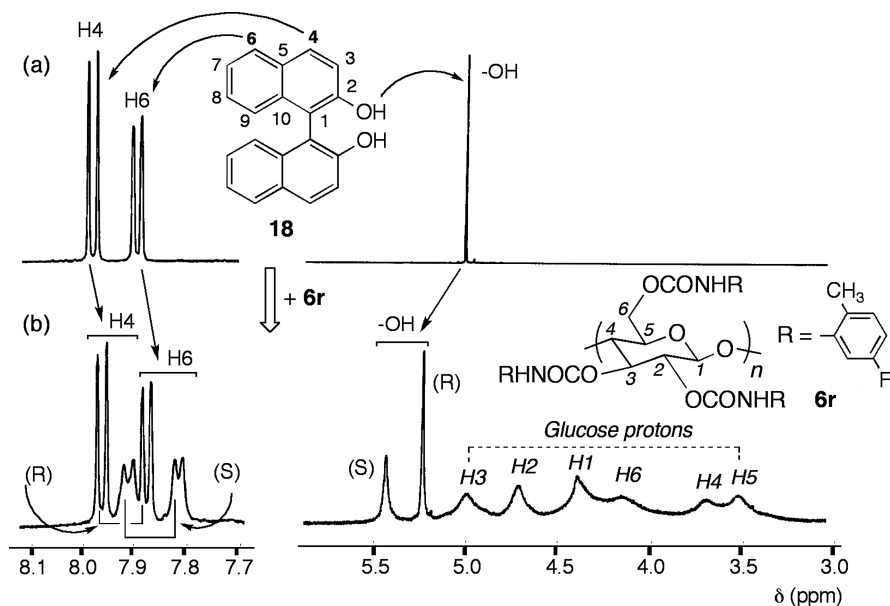


Fig. 12 ^1H NMR spectra of selected region of *rac*-1,1'-bi-2-naphthol **18** in the absence (a) and presence (b) of **6r** in CDCl_3 . Reprinted by permission from American Chemical Society [32]

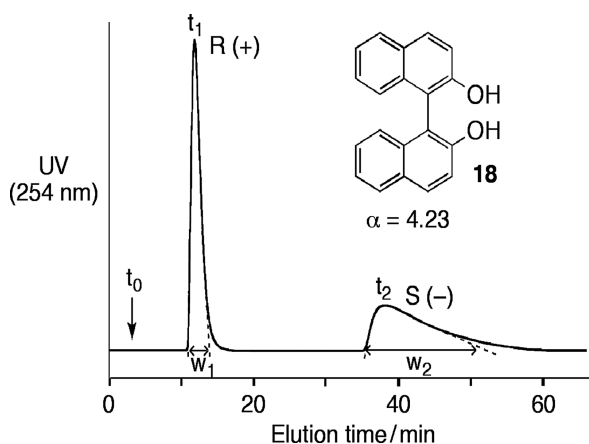


Fig. 13 Chiral separation of *rac*-**18**. CSP: cellulose 5-fluoro-2-methylphenylcarbamate **6r**. Column: 25×0.46 (i.d.) cm. Eluent: hexane/2-propanol (90/10). Flow rate: 1.0 ml/min. Reprinted by permission from American Chemical Society [32]

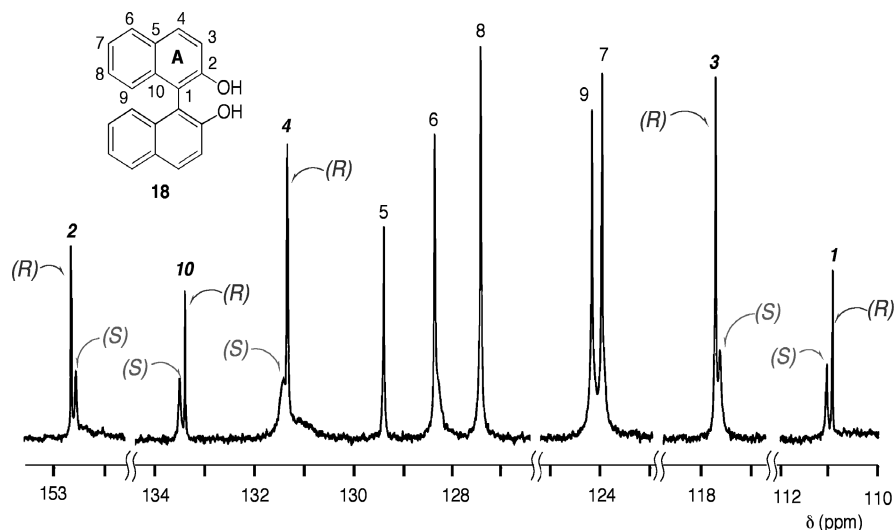


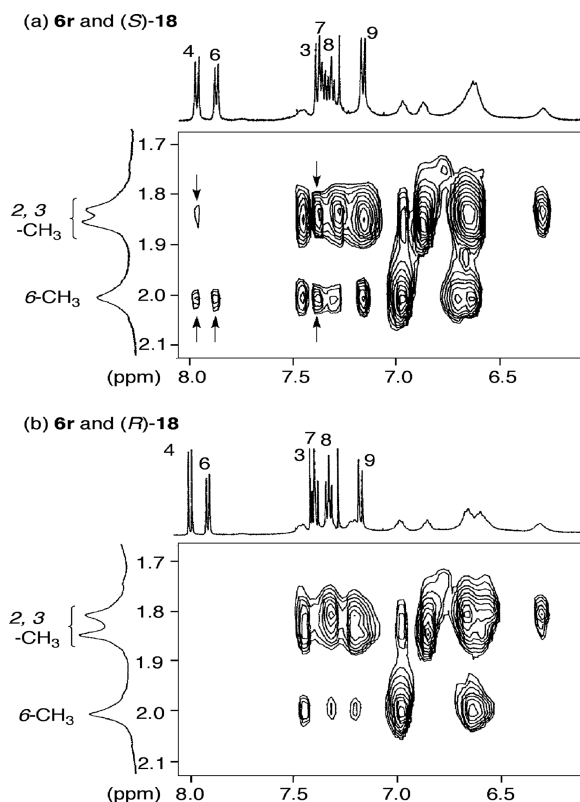
Fig. 14 ^{13}C NMR spectrum of *rac*-**18** in the presence of **6r** in CDCl_3 . Reprinted by permission from American Chemical Society [32]

The chiral recognition can also be observed by ^{13}C NMR spectroscopy. Figure 14 shows the recognition of the enantiomers **18** by ^{13}C NMR spectroscopy [32]. The resonances of the C1–C4 and C10 carbons of **18**, which are located near the hydroxy groups, are separated into enantiomers in the presence of **6r**, and the carbon resonances of (*S*)-**18** clearly become broader than that of (*R*)-**18** as well as the observation in the ^1H NMR spectrum. This indicates that ring A of (*S*)-**18** may be favorably located in the chiral groove of **6r**. Measurements of the relaxation time also support this speculation.

In addition, the ^1H NMR titrations of **6r** with (*S*)- and (*R*)-**18** and a Job plot of the continuous changes in the chemical shifts for the complex **6r**–(*S*)-**18** were conducted in order to investigate the binding sites of **6r** and the stoichiometry of the complexation [32]. The Job plot denotes that the maximum complex formation occurs at around 0.5 mol fraction of the glucose unit of **6r**. This represents that each glucose unit of **6r** may have the same binding affinity to (*S*)-**18** probably due to the regular structure of **6r** even in a solution state. During the titrations, the H2 proton resonance of a glucose unit is dramatically upfield shifted as the concentration of (*S*)-**18** increases, while the other glucose proton resonances only move slightly. This upfield shift of the H2 proton resonance implies that the H2 proton may be located above the naphthyl ring of (*S*)-**18**.

More valuable information on the binding geometry and dynamics between the polysaccharide derivatives and the enantiomers can be obtained from the intermolecular nuclear Overhauser effects (NOE). Figure 15 shows the NOE spectroscopy (NOESY) spectra of **6r**–(*S*)-**18** (a) and **6r**–(*R*)-**18** (b) in the region related to the methyl protons on the phenyl group of **6r** and the aromatic protons of **18** [32]. Clear intermolecular NOE cross-peaks shown by the arrows could be observed

Fig. 15 500 MHz expanded NOESY spectra at a mixing time of 300 ms of the mixtures of (a) **6r** and (*S*)-**18** and (b) **6r** and (*R*)-**18** in the region between the aromatic protons (**6r** and **18**) and the methyl protons on the phenyl groups of **6r** in CDCl₃ at 30°C. Reprinted by permission from American Chemical Society [32]



between the methyl proton of **6r** and the aromatic protons H4, H6, and H7 of (*S*)-**18** (Fig. 15a). On the other hand, the mixture of **6r** and (*R*)-**18** exhibited no intermolecular NOE cross-peaks (Fig. 15b), probably due to a weaker interaction. These results indicate that (*S*)-**18** more strongly binds or interacts with **6r** than (*R*)-**18**, and the naphthyl protons of (*S*)-**18** are closely located to the glucose proton of **6r** within less than 5 Å. These observations correspond to the results of the HPLC and 1D NMR experiments. Based on the HPLC and NMR data combined with the structural data for the cellulose phenylcarbamate (**6f**) determined by X-ray analysis, a computational structure has been proposed for the **6r**–(*S*)-**18** complex (Fig. 16) [32]. This calculation model shows that two hydroxy protons of (*S*)-**18** interact with the carbonyl oxygens of the carbamate groups of **6r** through hydrogen bonding.

Recently, Wirth et al. explained the enantioselective interaction between amylose 3,5-dimethylphenylcarbamate **7p** and the *O*-*tert*-butyltyrosine allyl ester **19** (Fig. 17) using the intermolecular NOEs [34]. The major differences in the NOESY cross-peaks between the D- and L-isomers are observed in the aromatic region of **19**. Compared to the D-**19**, the greater number and stronger intensity of the NOESY cross-peaks were observed between the aromatic protons of L-**19** and the glucose protons of **7p** including the Ha-H2, Ha-H3, Ha-H5, Hb-H2, Hb-H3, and Hb-H5

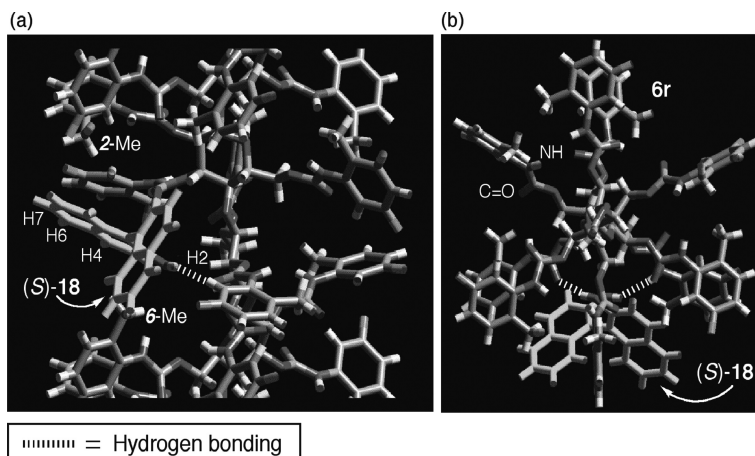


Fig. 16 Calculated structure of the complex **6r**-(*S*)-**18**. (a) View along the helix axis and (b) perpendicular to the helix axis. Reprinted by permission from American Chemical Society [32]

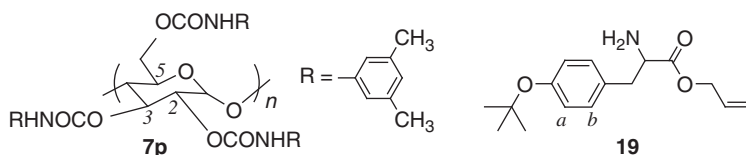


Fig. 17 Structures of amylose 3,5-dimethylphenylcarbamate **7p** and *O*-*tert*-butyltyrosine allyl ester **19**

pairs. This result indicates that the L-**19** exists in closer proximity to the chiral groove in **7p** than the D-**19**. This structural relationship allows a stronger interaction between the L-**19** and **7p**. The mechanistic study by NMR is well amenable to the HPLC separation results.

4.2 Computational Methods

The chiral recognition mechanism of small molecule-based CSPs has been extensively investigated from theoretical viewpoints, especially by Lipkowitz et al. [35–37]. The interaction energies between the CSPs and enantiomers were calculated by molecular-mechanics (MM), molecular-dynamics (MD), and quantum-mechanical calculations, and the rational interaction models between the CSPs and racemates have been proposed. Until now, several attempts have also been carried out for the qualitative understanding of the chromatographic behavior of the polysaccharide-based CSPs.

The interaction energy calculations between the phenylcarbamate **6f** or 3, 5-dimethylphenylcarbamate **6p** of cellulose and *trans*-stilbene oxide **10** or benzoin **13** were performed using various force fields [26, 38]. During a chromatographic resolution, **10** can be completely separated on both **6f** and **6p** ($\alpha = 1.46$) and ($\alpha = 1.68$). However, their elution orders are opposite; the (*R,R*)-isomer is first eluted on **6f**, and the (*S,S*)-isomer on **6p**. Meanwhile, **6p** can efficiently separate **13** ($\alpha = 1.58$), while **6f** cannot ($\alpha \approx 1$).

The applied calculations were roughly divided into the following two methods, which differ in these enantiomer generation methods. In one method, enantiomers were individually generated around the carbonyl oxygen and the NH proton of the carbamate group of **6f** and **6p** and rotated at 15° intervals for the *x*, *y*, and *z* axes. The interaction energy calculation was performed for each carbonyl oxygen and NH proton at the 2-, 3-, and 6-positions of the glucose units with all possible combinations of the rotation angles of the enantiomers. The calculation results are evaluated with the lowest interaction energy and the distribution of the interaction energy. In another method, enantiomers with a particular orientation were randomly generated by the Monte Carlo method on the surface of **6f** and **6p**, and then the interaction energy was estimated step by step through the MM calculation between the molecules [39]. In both calculations, the nonamers of **6f** and **6p** were used as chiral selectors, and the enantiomers were generated around the middle part of their structures in order to avoid the influence of the end groups.

Both calculation results well agreed with the chromatographic results. The averaged or lowest interaction energy between **6f** and (*S,S*)-**10** was lower than that between **6f** and (*R,R*)-**10**, while an opposite enantiomer preference was found in the **6p**–**10** system. In the case of **13**, almost no difference in the interaction energies with **6f** was observed for the enantiomers.

The interaction energy difference between the enantiomers was clearly recognized only when the enantiomers were generated in a chiral groove of **6f** and **6p**. This result indicates that the polar carbamate groups of these phenylcarbamate derivatives may be the most important chiral recognition site for polar racemates.

Figure 18 shows a graphical view of the interaction mode between **6f** and (*S,S*)-**10**, which has the lowest interaction energy obtained by the second calculation method [26]. (*S,S*)-**10** is interned inside **6f** through hydrogen bonding between the NH proton of the carbamate group of **6f** and the ether oxygen atom of (*S,S*)-**10**. In addition, each phenyl group of **10** may interact with the phenyl groups of **6f** through π – π interactions. Although the actual reason for the opposite enantioselectivity of **6f** and **6p** toward **10** is unknown, the different arrangement of aromatic groups in **6f** and **6p** is expected to be responsible for the reversed enantioselectivity.

Aboul-Enein et al. [40] and Grinberg et al. [41] also attempted molecular modeling to provide some insights into the chiral recognition mechanism of cellulose benzoate **4a** and cellulose 4-methylbenzoate **4b**, respectively. The molecular modeling of **4b** and (*R*)- and (*S*)-**20** (Fig. 19) suggests that hydrogen bonding is a primary factor for the separation, and the calculated energy values obtained from the molecular modeling are consistent with the chromatographic results [41].

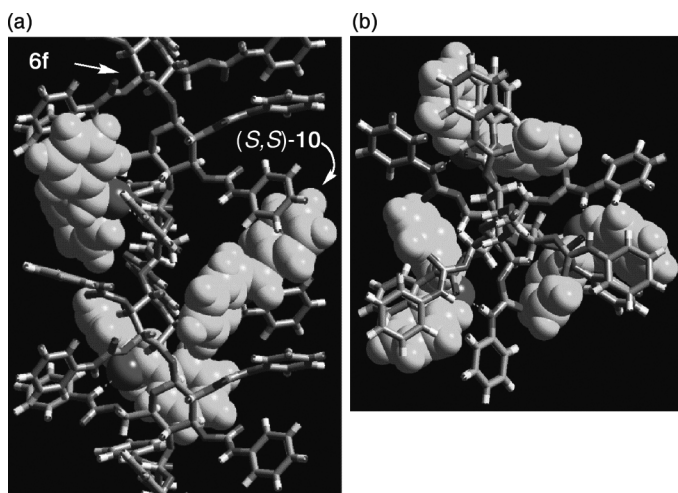
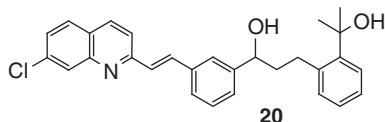


Fig. 18 Calculated structure of the complex **6f**–(*S,S*)-**10** formed through hydrogen bondings. (a) View along the helix axis and (b) perpendicular to the helix axis. Reprinted by permission from The Chemical Society of Japan [26]

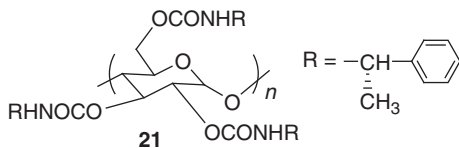
Fig. 19 Structure of racemate **20**



4.3 Other Studies for Chiral Recognition Mechanism

The difference in the enantioselective adsorption sites among the cellulose 3, 5-dimethylphenylcarbamate **6p**, amylose 3,5-dimethylphenylcarbamate **7p**, and amylose (*S*)-1-phenylethylcarbamate **21** (Fig. 20) was investigated by Franses et al. using attenuated total reflection infrared (ATR-IR) spectroscopy, X-ray diffraction (XRD), ^{13}C cross-polarization/magic-angle spinning (CP/MAS) and MAS solid-state NMR, and density functional theory (DFT) modeling [42]. The ATR-IR results show that the strengths of the hydrogen bond of the carbamate groups in these polymers are significantly different. Compared to **7p**, **6p** has a weaker intramolecular

Fig. 20 Structure of amylose (*S*)-1-phenylethylcarbamate **21**



hydrogen bonding mainly due to the differences in the backbones. Therefore, the chiral groove of **6p** is expected to be slightly larger than that of **7p**. For **21**, on the other hand, the hydrogen-bonding interaction of the carbonyl groups becomes stronger than **7p** due to the additional interactions with the benzyl proton in the same side chains. The XRD results suggest that the packing arrangements are different among the three derivatives, resulting in different nanostructures of the chiral grooves. Based on the CP/MAS NMR, it is inferred that the conformations of the backbone glycoside linkages are similar in **7p** and **21**, but different in **6p** and **7p**. DFT simulations predict that the **6p** and **7p** side chains have a planar conformation, while the side chain of **21** is nonplanar, and possibly has multiple conformations. They concluded that the carbonyl, NH, and phenyl groups of these polymers are expected to be oriented in different ways and that their carbamate groups show quite different interaction energies in their hydrogen bonding. This may be the major factor affecting the selectivity of the chiral analytes.

In order to clarify the role of the eluents in the chiral separation on polysaccharide derivatives, Franses et al. systematically investigated the interaction between **7p** and various organic solvents used as eluents by the above analytical method [43–45]. The polar solvents, such as methanol, ethanol, 2-propanol, or acetonitrile, change in the hydrogen-bonding states of the carbonyl and NH groups in **7p**, and seem to cause changes in the polymer crystallinity and side-chain mobility. On the other hand, the polymer structure remains essentially unchanged upon absorption of the nonpolar hexane. Wang et al. also studied the effects of the eluent on the structure and chiral recognition of **7p** by solid-state NMR [27, 46, 47]. These results indicated that the branched alcohols, such as 2-propanol and *t*-butyl alcohol, caused more twisting of the glucose units on the helical structure than the linear alcohols, such as ethanol, 1-propanol, and 1-butanol. These structural differences in **7p** may cause a change in the recognition ability in various eluents including different types of alcohol modifiers.

Recently, the conformational changes of **7p** in the presence of polar solvents were investigated using solid-state vibrational circular dichroism (VCD) spectroscopy by Grinberg et al. [48]. The VCD results revealed that the conformations of **7p** are drastically changed depending on the concentration of the alcohols, such as ethanol and 2-propanol, in the polymer film. These conformation changes seem to affect the chiral recognition.

5 Conclusions

In this chapter, the development and chiral recognition mechanism of polysaccharide-based CSPs for the efficient chromatographic separation of enantiomers have been outlined. The recognition abilities of native polysaccharides are not sufficient for use as CSPs, but their abilities can be substantially improved by the proper modifications of their structures. At present, more than 10 kinds of polysaccharide-based CSPs are commercially available and practically used around the world as

CSPs for liquid chromatography due to their high-recognition ability and high loading capacity for a the wide range of racemates. Until now, the chiral recognition mechanism of the polysaccharide derivatives has been clarified to some extent by X-ray analysis, spectroscopic analysis, and computational methods. Further understanding of the chiral recognition mechanism on a molecular level will help with the prediction of the separability of enantiomers and the development of more efficient CSPs based on the polysaccharide derivatives.

References

1. Rogozhin SV, Davankov VA (1971) Ligand chromatography on asymmetric complex-forming sorbents as a new method for resolution of racemates. *J Chem Soc Chem Commun* 490–493
2. Okamoto Y, Ikai T (2008) Chiral HPLC for efficient resolution of enantiomers. *Chem Soc Rev* 37:2593–2608
3. Subramanian G (ed) (2007) Chiral separation techniques: a practical approach, 3rd completely revised and updated edn. Wiley-VCH, Weinheim
4. Taylor DR, Maher K (1992) Chiral separations by high-performance liquid chromatography. *J Chromatogr Sci* 30:67–85
5. Pirkle WH, Pochapsky TC (1989) Considerations of chiral recognition relevant to the liquid-chromatographic separation of enantiomers. *Chem Rev* 89:347–362
6. Armstrong DW (1987) Optical isomer separation by liquid-chromatography. *Anal Chem* 59:84A–91A
7. Yamamoto C, Okamoto Y (2004) Optically active polymers for chiral separation. *Bull Chem Soc Jpn* 77:227–257
8. Nakano T (2001) Optically active synthetic polymers as chiral stationary phases in HPLC. *J Chromatogr A* 906:205–225
9. Chen XM, Yamamoto C, Okamoto Y (2007) Polysaccharide derivatives as useful chiral stationary phases in high-performance liquid chromatography. *Pure Appl Chem* 79:1561–1573
10. Kotake M, Sakan T, Nakamura N, Senoh S (1951) Resolution into optical isomers of some amino acids by paper chromatography. *J Am Chem Soc* 73:2973–2974
11. Dalglish C (1952) The optical resolution of aromatic amino-acids on paper chromatograms. *J Chem Soc* 3940–3942
12. Hess H, Burger G, Musso H (1978) Complete enantiomer separation by chromatography on potato starch. *Angew Chem Int Ed* 17:612–614
13. Hesse G, Hagel R (1973) A complete separation of a racemic mixture by elution chromatography on cellulose triacetate. *Chromatographia* 6:277–280
14. Okamoto Y, Kawashima M, Yamamoto K, Hatada K (1984) Useful chiral packing materials for high-performance liquid chromatographic resolution cellulose triacetate and tribenzoate coated on macroporous silica gel. *Chem Lett* 13:739–742
15. Ichida A, Shibata T, Okamoto Y, Yuki Y, Namikoshi H, Toda Y (1984) Resolution of enantiomers by HPLC on cellulose derivatives. *Chromatographia* 19:280–284
16. Okamoto Y, Aburatani R, Hatada K (1987) Chromatographic chiral resolution XIV- cellulose tribenzoate derivatives as chiral stationary phases for high-performance liquid chromatography. *J Chromatogr* 389:95–102
17. Okamoto Y, Kaida Y (1994) Resolution by high-performance liquid chromatography using polysaccharide carbamates and benzoates as chiral stationary phases. *J Chromatogr A* 666:403–419
18. Yashima E, Yamamoto C, Okamoto Y (1998) Polysaccharide-based chiral LC columns. *Synlett* 344–360

19. Okamoto Y, Kawashima M, Hatada K (1984) Useful chiral packing materials for high-performance liquid chromatographic resolution of enantiomers: phenylcarbamates of polysaccharides coated on silica gel. *J Am Chem Soc* 106:5357–5359
20. Okamoto Y, Kawashima M, Hatada K (1986) Controlled chiral recognition of cellulose triphenylcarbamate derivatives supported on silica gel. *J Chromatogr* 363:173–186
21. Okamoto Y, Ohashi T, Kaida Y, Yashima E (1993) Resolution of enantiomers by HPLC on tris(4-alkoxyphenylcarbamate)s of cellulose and amylase. *Chirality* 5:616–621
22. Chankvetadze B, Yashima E, Okamoto Y (1994) Chloromethylphenylcarbamate derivatives of cellulose as chiral stationary phases for high-performance liquid chromatography. *J Chromatogr A* 670:39–49
23. Okamoto Y, Aburatani R, Fukumoto T, Hatada K (1987) Useful chiral stationary phases for HPLC amylose tris(3,5-dimethylphenylcarbamate) and tris(3,5-dichlorophenylcarbamate) supported on silica gel. *Chem Lett* 16:1857–1860
24. Chankvetadze B, Yashima E, Okamoto Y (1995) Dimethyl-, dichloro- and chloromethylphenylcarbamates of amylose as chiral stationary phases for HPLC. *J Chromatogr A* 694:101–109
25. Yashima E, Yamamoto C, Okamoto Y (1995) Enantioseparation on fluoro-methylphenylcarbamates of cellulose and amylose as chiral stationary phases for HPLC. *Polym J* 27:856–861
26. Yamamoto C, Yashima E, Okamoto Y (1999) Computational studies on chiral discrimination mechanism of phenylcarbamate derivatives of cellulose. *Bull Chem Soc Jpn* 72:1815–1825
27. Wenslow RM, Wang T (2001) Solid-state NMR characterization of amylose tris(3,5-dimethylphenylcarbamate) chiral stationary-phase structure as a function of mobile-phase composition. *Anal Chem* 73:4190–4195
28. Yamamoto C, Yashima E, Okamoto Y (2002) Structural analysis of amylose tris(3,5-dimethylphenylcarbamate) by NMR relevant to its chiral recognition mechanism in HPLC. *J Am Chem Soc* 124:12583–12589
29. Yashima E, Yamada M, Okamoto Y (1994) An NMR study of chiral recognition relevant to the liquid chromatographic separation of enantiomers by a cellulose derivative. *Chem Lett* 23:579–582
30. Yashima E, Yamada M, Yamamoto C, Nakashima M, Okamoto Y (1997) Chromatographic enantioseparation and chiral discrimination in NMR by trisphenylcarbamate derivatives of cellulose, amylose, oligosaccharides, and cyclodextrins. *Enantiomer* 2:225–240
31. Okamoto Y, Yashima E, Yamamoto C (1997) NMR studies of chiral discrimination by phenylcarbamate derivatives of cellulose. *Macromol Symp* 120:127–137
32. Yashima E, Yamamoto C, Okamoto Y (1996) NMR studies of chiral discrimination relevant to the liquid chromatographic enantioseparation by a cellulose phenylcarbamate derivative. *J Am Chem Soc* 118:4036–4048
33. Kubota T, Yamamoto C, Okamoto Y (2002) Chromatographic enantioseparation by cycloalkylcarbamate derivatives of cellulose and amylase. *Chirality* 14:372–376
34. Ye YK, Bai S, Vyas S, Wirth MJ (2007) NMR and computational studies of chiral discrimination by amylose tris(3,5-dimethylphenylcarbamate). *J Phys Chem B* 111:1189–1198
35. Lipkowitz KB (1994) Modeling Enantiodifferentiation in chiral chromatography. In: Subramanian G (ed) *A Practical Approach to Chiral Separations by Liquid Chromatography*. Wiley-VCH, New York
36. Lipkowitz KB (1995) Theoretical studies of type II–V chiral stationary phases. *J Chromatogr A* 694:15–37
37. Lipkowitz KB (2001) Atomistic modeling of enantioselection in chromatography. *J Chromatogr A* 906:417–442
38. Yashima E, Yamada M, Kaida Y, Okamoto Y (1995) Computational studies on chiral discrimination mechanism of cellulose trisphenylcarbamate. *J Chromatogr A* 694:347–354
39. Theodorou DN, Suter UW (1985) Detailed molecular structure of a vinyl polymer glass. *Macromolecules* 18:1467–1478

40. Aboul-Enein HY, Ali I, Laguerre M, Felix G (2002) Molecular modeling of enantiomeric resolution of methylphenidate on cellulose tris benzoate chiral stationary phase. *J Liq Chromatogr Relat Technol* 25:2739–2748
41. O'Brien T, Crocker L, Thompson R, Thompson K, Toma PH, Conlon DA, Feibush B, Moeder C, Bicker G, Grinberg N (1997) Mechanistic aspects of chiral discrimination on modified cellulose. *Anal Chem* 69:1999–2007
42. Kasat RB, Wang NHL, Franses EI (2007) Effects of backbone and side chain on the molecular environments of chiral cavities in polysaccharide-based biopolymers. *Biomacromolecules* 8:1676–1685
43. Kasat RB, Zvinevich Y, Hillhouse HW, Thomson KT, Wang NHL, Franses EI (2006) Direct probing of sorbent-solvent interactions for amylose tris(3,5- dimethylphenylcarbamate) using infrared spectroscopy, X-ray diffraction, solid-state NMR, and DFT modeling. *J Phys Chem B* 110:14114–14122
44. Kasat RB, Chin CY, Thomson KT, Franses EI, Wang NHL (2006) Interpretation of chromatographic retentions of simple solutes with an amylose-based sorbent using infrared spectroscopy and DFT modeling. *Adsorption* 12:405–416
45. Kasat RB, Wang NHL, Franses EI (2008) Experimental probing and modeling of key sorbent-solute interactions of norephedrine enantiomers with polysaccharide-based chiral stationary phases. *J Chromatogr A* 1190:110–119
46. Wang T, Wenslow RM (2003) Effects of alcohol mobile-phase modifiers on the structure and chiral selectivity of amylose tris(3,5-dimethylphenylcarbamate) chiral stationary phase. *J Chromatogr A* 1015:99–110
47. Helmy R, Wang T (2005) Selectivity of amylose tris(3,5-dimethylphenylcarbamate) chiral stationary phase as a function of its structure altered by changing concentration of ethanol or 2-propanol mobile-phase modifier. *J Sep Sci* 28:189–192
48. Ma SL, Shen S, Lee H, Yee N, Senanayake C, Nafie LA, Grinberg N (2008) Vibrational circular dichroism of amylose carbamate: structure and solvent-induced conformational changes. *Tetrahedron Asymmetry* 19:2111–2114



<http://www.springer.com/978-3-642-12444-0>

Chiral Recognition in Separation Methods
Mechanisms and Applications

Berthod, A. (Ed.)

2010, XIV, 337 p., Hardcover

ISBN: 978-3-642-12444-0